a proper accounting of counterion effects and polyelectrolyte coil expansion might help explain the observed behaviors. In this regard it may be useful to compare the conformation and mobility of the identical samples both in free solution and in a gel medium.

Acknowledgment. We gratefully acknowledge the National Science Foundation Materials Research Laboratory at the University of Massachusetts for financial support; we also thank Prof. Muthukumar of the University of Massachusetts for his helpful comments.

Registry No. Agarose, 9012-36-6.

References and Notes

(1) Andrews, A. T. *Electrophoresis: Theory, Techniques, and Biochemical and Clinical Applications*; Oxford University Press: New York, 1986.
(2) Chen, J.-L.; Morawetz, H. *Macromolecules* **1982**, *15*, 1185–1188.
(3) Serwer, P. *Electrophoresis (Weinheim, Fed. Repub. Germ.)* **1983**, *4*, 375–382.
(4) Stellwagen, N. C. *Biopolymers* **1985**, *24*, 2243–2255.
(5) Giddings, J. C. In *Advances in Chromatography*; Giddings, J. C., Grushka, E., Cazes, J., Brown, P. R., Eds.; Marcel-Dekker: Washington, DC, 1982; Vol. 20, pp 217–254.
(6) Muller, G.; Yonnet, C. *Makromol. Chem., Rapid Commun.* **1984**, *5*, 197–201.
(7) Lerman, L. S.; Frisch, H. L. *Biopolymers* **1982**, *21*, 995–997.
(8) Lumpkin, O. J.; Zimm, B. H. *Biopolymers* **1982**, *21*, 2315–2316.
(9) Lumpkin, O. J.; Dejardin, P.; Zimm, B. H. *Biopolymers* **1985**, *24*, 1573–1593.
(10) Slater, G. W.; Noolandi, J. *Phys. Rev. Lett.* **1985**, *55*, 1579–1582.
(11) Slater, G. W.; Noolandi, J. *Biopolymers* **1986**, *25*, 431–454.
(12) Adolf, D. *Macromolecules* **1987**, *20*, 116–121.
(13) Lumpkin, O. J. *J. Chem. Phys.* **1984**, *81*, 5201–5205.
(14) Edmondson, S. P.; Gray, D. M. *Biopolymers* **1984**, *23*, 2725–2742.
(15) Hervet, H.; Bean, C. P. *Biopolymers* **1987**, *26*, 727–742.
(16) Davis, R. M.; Russel, W. B. *Macromolecules* **1987**, *20*, 518–525.
(17) Davis, R. M.; Russel, W. B. *J. Polym. Sci., Part B: Polym. Phys.* **1986**, *24*, 511.
(18) Rodbard, D.; Chrambach, A. *Proc. Natl. Acad. Sci. U.S.A.* **1970**, *65*, 970–977.
(19) Hermans, J. J. *J. Polym. Sci.* **1955**, *18*, 527–534.
(20) Hermans, J. J.; Fujita, H. *Proc. K. Ned. Akad. Wet., Ser. B: Phys. Sci.* **1955**, *B58*, 182–187.
(21) Vink, H. *Makromol. Chem.* **1981**, *182*, 279–281.
(22) Noolandi, J.; Rousseau, J.; Slater, G. W.; Turmel, C.; Lalande, M. *Phys. Rev. Lett.* **1987**, *58*, 2428–2431.
(23) Manning, G. S. *J. Chem. Phys.* **1969**, *51*, 924–933.
(24) Manning, G. S. *Annu. Rev. Phys. Chem.* **1972**, *23*, 117–137.
(25) Russel, W. B. *J. Polym. Sci., Polym. Phys. Ed.* **1982**, *20*, 1233–1247.
(26) Whitlock, L. R. In *New Directions in Electrophoretic Methods*; Jorgenson, J. W., Phillips, M., Eds.; ACS Symposium Series 335; American Chemical Society: Washington, DC, 1987; pp 222–245.
(27) Zimm, B. H. In *Coulombic Interactions in Macromolecular Systems*; Eisenberg, A., Bailey, F. E., Eds.; ACS Symposium Series 302; American Chemical Society: Washington, DC, 1986; pp 212–215.
(28) Rodriguez, F. *Principles of Polymer Systems*; McGraw-Hill; New York, 1982; pp 132–134.
(29) Fangman, W. L. *Nucleic Acids Res.* **1978**, *5*, 653–665.
(30) A linear correlation of the logarithim of mobility with agarose concentration is often observed in DNA and protein electrophoresis.[1] No theoretical basis for such a correlation is yet available for flexible polymers, and our data are not more linear on a log–linear plot than on the linear–linear plot of Figure 6.
(31) Olivera, B. M.; Baine, P.; Davidson, N. *Biopolymers* **1964**, *2*, 245–257.
(32) Nagasawa, M.; Noda, I.; Takahashi, T.; Shimamoto, N. *J. Phys. Chem.* **1972**, *76*, 2286–2294.
(33) Noda, I.; Nagasawa, M.; Ota, M. *J. Am. Chem. Soc.* **1964**, *86*, 5075–5079.
(34) Ross, P. D.; Scruggs, R. L. *Biopolymers* **1964**, *2*, 231–236.
(35) Imai, N.; Iwasa, K. *Isr. J. Chem.* **1973**, *11*(2–3), 223–233.
(36) Nagasawa, M.; Soda, A.; Kagawa, I. *J. Polym. Sci.* **1958**, *31*, 439–451.

Force between Surfaces That Confine a Polymer Solution: Derivation from Self-Consistent Field Theories

Evan A. Evans

Departments of Pathology and Physics, University of British Columbia, Vancouver, British Columbia, Canada V6T 1W5. *Received October 24, 1988*

ABSTRACT: Self-consistent field (SCF) theory for an incompressible polymer solution confined between parallel surfaces predicts the existence of a nonuniform hydrostatic pressure field to maintain the density constraint. The hydrostatic field is a local isotropic stress given by the excess chemical potential of the solvent relative to the adjacent bulk solution plus effects of nonlocal interactions between solvent and polymer segments. Based on the mechanical work to displace the surfaces, mean-field analysis of the polymer solution as a continuum also leads to the definition of a local deviatoric (shear) stress, which is derived from the equivalence of interfacial tension and the excess free energy of the gap solution (per unit area) established by SCF theory. The deviatoric stress arises from restricted equilibrium effects and nonlocal interactions. The sum of isotropic and deviatoric stress components defines the local axial stress aligned along the coordinate normal to the surfaces. The incremental work to displace surfaces with constant cross-sectional area yields the force per unit area on each surface, which reduces to the axial stress evaluated at the *midpoint* of the gap. For complete equilibrium without nonlocal effects, the force per unit area is simply given by the excess chemical potential of the solvent (relative osmotic pressure) at the center of the gap. The work per unit area (interaction potential) to assemble the surfaces from large separation to stable contact is the integral of the force per unit area over the full range of displacement. It is shown that changes in the interaction potential differ from changes in the excess free energy per unit area of the gap by the cumulated value of the change in stress field with respect to displacement (analogous to the $V\,dP$ term associated with the change in a Gibbs potential). This leads to a longer range interaction between surfaces than that predicted by the distance dependence of the excess free energy. Experimental data for interaction potentials between phospholipid bilayer surfaces in concentrated aqueous solutions of large nonadsorbent polymers correlate well with predictions of the mean-field analysis.

I. Introduction

Thirty years ago, Mackor and van der Waals analyzed the excess free energy of a solution of dimeric molecules confined between rigid surfaces.[1] Since then, self-consistent field (SCF) theories have been developed to predict excess free energy of polymer solutions confined between rigid surfaces. Both lattice mean-field models[2] and continuous space approximations[3,4] have been used to derive

0024-9297/89/2222-2277$01.50/0

the excess free energy for the gap solution relative to a solution with the same volume and fixed reference composition. A key extension of these analyses has been to assume that the interaction potential (i.e., the work per unit area to assemble the surfaces from infinity to a specific distance) is the excess free energy per unit area of the gap minus the value for two surfaces at infinite separation. The force per unit area on each surface is then taken as the derivative of this interfacial free energy density with respect to separation. However, the approach appears to require a correction, because there is a nonuniform pressure distribution implicit in the mean-field analysis which has been overlooked. The pressure is a hydrostatic field that arises from the requirement of local incompressibility. Although they did not identify this field as a physical stress, Hong and Noolandi[4] carefully derived a set of self-consistent fields based on the statistical mechanics of polymer random walks in mean fields for an incompressible solution and showed that a Lagrange multiplier is required to enforce the density constraint (i.e., local mean-field pressure). Similarly in earlier derivations by Helfand and Sapse,[4] local compressibility was considered and resulted in a density-dependent field that can be interpreted as a local mean-field pressure. The negative of pressure defines the local isotropic stress in the solution. As will be shown in this paper, the differential work to increase the separation between surfaces is dominated by the integral over the gap region of the isotropic stress × local volume dilatation when the polymer chains are in complete equilibrium with the adjacent bulk reservoir. Further analysis shows that the differential work (surface force × displacement) is equal to the change of the excess free energy of the gap solution *reduced* by the integral over the gap region of the change of the isotropic stress field with respect to change in gap dimension. This is analgous to extracting the volume × pressure change from the change in Gibbs potential to obtain the incremental work to displace applied forces. The principal consequence of the adjustment is to create a longer range interaction between surfaces (i.e., slower rate of decay of the force). Further, the force per unit area on the surfaces (in the absence of nonlocal effects) is given simply by the osmotic pressure difference (bulk solution − gap solution) evaluated at the *midpoint* of the gap, a la Langmuir.

First, the SCF theory for incompressible homopolymer–solvent solutions will be briefly summarized on the basis of extensive previous developments[4] and used to derive the mean-field prescription for local relative pressure. Next, mean-field predictions will be obtained for the local axial stress field (sum of isotropic and deviatoric components) from the mechanical work of deformation of the polymer solution associated with displacement of the surfaces. It is shown that the force per unit area on each surface is the axial stress evaluated at the center of the gap. The integral of the force per unit area from infinite separation to stable contact defines the interaction potential (energy per unit area). Finally, experimental data for interaction potentials between phospholipid bilayer surfaces in aqueous solutions of large nonadsorbent polymers will be used to support the predictions of this analysis in semidilute/good solvent conditions where polymer depletion forces cause strong adhesion of the membranes.

II. Self-Consistent Fields for Homopolymer–Solvent Solutions

The approach used to establish the excess free energy is based on the partition function for polymer configurations derived from random walks of polymer segments in optimal mean-field potentials subject to appropriate boundary conditions at surface(s).[2-4] Here, developments of several references[4] will be abstracted and reduced to the essential relations leaving out many important details. To start with, it is assumed that effects of inhomogeneities can be accounted for by a set of position-dependent fields $\epsilon_k(\vec{x})$ which act on individual components of the solution (k = particular homopolymer or k = s for the solvent). These fields augment the free energy density $\tilde{F}_H$ of a homogeneous solution evaluated at the local composition to give the free energy density $\tilde{F}$ of the inhomogeneous solution as

$$\tilde{F} = \tilde{F}_H + \sum_k c_k \epsilon_k \tag{2.1}$$

where c_k are the local concentrations (number of particles per volume). For each polymer component, c_k is the concentration of segments at position $\vec{x}$; c_k/N_k is the local concentration of a polymer with N_k segments. Clearly, the local chemical potential (free energy per segment) μ_k of the kth component in the inhomogeneous solution is defined by

$$\mu_k = \mu_k^H + \epsilon_k \tag{2.2}$$

in terms of the chemical potential μ_k^H for a homogeneous solution at the local composition. The fields ϵ_k are made to be "self-consistent" through the free energy obtained for Gaussian random walks of the polymer components in related mean fields, $w_k(\vec{x})$. The unnormalized probability $q_k(\vec{x},\tau)$ of finding a chain section of fractional length τ with one end at $\vec{x}$ approximately satisfies a modified diffusion equation[4]

$$\frac{1}{N_k}\frac{\partial q_k}{\partial \tau} = \frac{a_k^2}{6}\nabla^2 q_k - \left(\frac{w_k}{kT}\right) q_k \tag{2.3}$$

where a_k is the statistical segment length (or random walk step size) and kT is Boltzmann's constant × temperature. Normalization leads to the concentration of the kth polymer component given by

$$\nu_k c_k = \int_0^1 d\tau\; q_k(\vec{x},\tau)\; q_k(\vec{x},1-\tau) \tag{2.4}$$

where ν_k is the volume per polymer segment (partial molecular volume) and $\nu_k c_k = \phi_k$ is the local volume fraction of the kth component. For the solvent, the mean-field potential is determined by its translational entropy:

$$w_s = -kT \ln (\nu_s c_s)$$

For the polymer components, the mean fields w_k are related to the free energy through the potential energy for segment–segment and segment–solvent interactions.

As originally introduced by Cahn and Hilliard,[4,7] the interaction energy for nonuniform regular solutions can be approximated by a gradient expansion in terms of the intermolecular potential energy $U_{kk'}(\vec{x}-\vec{x}')$ between unlike molecules (defined as zero between like molecules):

$$U(\vec{x}) \cong \frac{1}{2}\sum_{kk'} \bar{U}_{kk'} c_k c_{k'} + \frac{1}{12}\sum_{kk'} B_{kk'} c_k \nabla^2 c_{k'}$$

The zero moment

$$\bar{U}_{kk'} \equiv \int d^3x\; U_{kk'}(\vec{x}) \tag{2.5}$$

yields the classical Flory–Huggins[8] interaction parameters $\chi_{kk'}$ where $\bar{U}_{kk'} \equiv kT\chi_{kk'}\nu_{k'}$ is explicitly represented in the definition of the homogeneous free energy density, i.e., $\sum \bar{U}_{kk'} c_k c_{k'}$. The coefficients $B_{kk'}$ are the second moments of the intermolecular potential

$$B_{kk'} \equiv \int d^3x\; U_{kk'}(\vec{x})\; |\vec{x}|^2 \tag{2.6}$$

The nonlocal coefficients $B_{kk'}$ are often expressed as fractions of the Flory interaction parameters. With the expression for free energy derived from the partition function based on the interaction energy $U(\vec{x})$, self-consistency leads to the following relation between the fields ϵ_k and w_k:

$$\epsilon_k = -w_k - \left(\frac{kT}{N_k}\right) \ln \phi_k + \frac{1}{6}\sum_{k'} B_{kk'}\nabla^2 c_{k'} \qquad (2.7)$$

III. "Optimal" Self-Consistent Fields

The optimal set of self-consistent fields (ϵ_k, w_k) is obtained from minimization of the free energy subject to constraints. Variation of the free energy functional involves variations of the free energy in a local domain with respect to the number of molecules in that domain. Changing the number of molecules in a domain changes the size of the domain. Additional dilatation occurs when molecules are transported into—or out of—the domain due to physical displacement of boundaries. Procedures in continuum mechanics provide a useful way to handle this problem.[5] First, a reference geometry is defined where the element domain sizes are given by d^3x_0. The measure of dilatation is the local volume ratio $\lambda = d^3x/d^3x_0$. Thus, the extensive numbers of molecules $\tilde{n}_k$ (segments or solvent) in a reference domain are explicitly given by

$$\tilde{n}_k \equiv \frac{dn_k}{d^3x_0} = \left(\frac{d^3x}{d^3x_0}\right)\frac{dn_k}{d^3x} = \lambda c_k \qquad (3.1)$$

with the obvious corollary

$$\lambda \equiv \sum_k \nu_k \tilde{n}_k \qquad (3.2)$$

Likewise, the extensive free energy in a local domain is

$$\tilde{F}\, d^3x = (\tilde{F}\lambda)\, d^3x_0 \qquad (3.3)$$

Therefore, the local chemical potential is obtained by

$$\frac{d(\tilde{F}\lambda)}{d\tilde{n}_k} = \mu_k \qquad (3.4)$$

[Derivatives $d()/dn_i$ can be expressed in terms of derivatives with respect to concentrations through the relation

$$\frac{d()}{d\tilde{n}_i} \equiv \sum_k (\delta_{ik} - \nu_i c_k)\frac{\partial()}{\partial c_k} + \nu_i \frac{\partial()}{\partial \lambda} \qquad (3.5)$$

as derived from eq 3.1.]

The advantage of this approach is that variations of functionals can be treated as integrals of local variations as follows

$$\delta \int () \, d^3x \equiv \int \delta[\lambda()] \, d^3x_0 \qquad (3.6)$$

where the integrals are taken over the reference coordinates.

In the mean-field approximation, the solution confined between the surfaces is evaluated as a continuum. If the boundaries are stationary, mechanical equilibrium is given by the variational statement

$$\delta F + \int (p\delta\lambda)\, d^3x_0 \equiv 0 \qquad (3.7)$$

where $-p(\vec{x})$ is the local isotropic stress or negative hydrostatic pressure.[9] If the solution was compressible, then the pressure would be approximated by a constitutive relation (equation of state)

$$p = p_0 - K_B(\lambda - 1) + \ldots$$

where K_B is the elastic modulus for volume dilatation (compressibility^{-1}) of the mixture. Here, the polymer solution is treated as incompressible ($K_B \to \infty$, $\lambda \to 1$); thus, pressure becomes an arbitrary local stress (Lagrange multiplier) sufficient to guarantee mechanical equilibrium in eq 3.7 and incompressibility.

For a polymer solution between surfaces bounded by a bulk reference solution, another relation must be introduced to characterize the (open or restricted) exchange of molecules between gap and bulk regions. Conservation of components is given by

$$\int_{gap} \delta\tilde{n}_k \, d^3x_0 \equiv -\delta n_k{}^B$$

where the superscript B represents reference solution properties at composition $n_k{}^B$. If the gap is in equilibrium with a very large bulk region, the bulk region becomes a constant chemical potential reference state, which leads to

$$\int_{gap} [\delta(\tilde{F}\lambda) - \sum_k \mu_k{}^B \delta\tilde{n}_k + (p - p_B)\delta\lambda] \, d^3x_0 = 0 \qquad (3.8)$$

from eq 3.7. The first two terms in this equation are the variation in local *excess* free energy, and the last term represents the virtual work associated with local dilation × the relative pressure between positions in the gap and bulk region. For incompressible solutions (ν_k = constants), eq 3.8 yields a set of equations for local chemical potentials

$$(\mu_k{}^H + \epsilon_k - \mu_k{}^B) + (p - p_B)\nu_k = 0$$

since $\delta\lambda/\delta\tilde{n}_k = \nu_k$ from eq 3.2. If exchange of polymer between gap and bulk regions is restricted, then additional constraint equations are specified

$$n_k{}^g \equiv n_k - n_k{}^e$$

where $n_k{}^g$ are fixed numbers of molecules required in the gap; $n_k{}^e$ are the numbers of molecules expected to be in the gap at complete equilibrium. These constraints only restrict the polymer components (solvent is assumed to be freely exchangeable) and are guaranteed by the introduction of global Lagrange multipliers g_k conjugate to each constraint equation. As such, the local chemical potential of a particular polymer component will include a Lagrange multiplier as follows:

$$(\mu_k{}^H + \epsilon_k + g_k - \mu_k{}^B) + (p - p_B)\nu_k = 0 \qquad (3.9)$$

The equation (k = s) for the solvent is left unchanged (i.e., $g_s = 0$).

Equations 3.9 define the *optimal* self-consistent fields w_k through eq 2.7

$$0 = (\mu_k{}^H - \mu_k{}^B + g_k) - w_k - \left(\frac{kT}{N_k}\right) \ln \phi_k + \frac{1}{6}\sum_{k'} B_{kk'}\nabla^2 c_{k'} + (p - p_B)\nu_k \qquad (3.10)$$

The local pressure is obtained directly from the equation for the solvent component and the solvent mean field, $w_s \equiv -kT \ln \phi_s$

$$(p_B - p) = \frac{(\mu_s{}^H - \mu_s{}^B)}{\nu_s} + \frac{1}{6}\sum_{k'} \frac{B_{sk'}}{\nu_s}\nabla^2 c_{k'} \qquad (3.11)$$

Hence, the optimal mean fields for the polymer components reduce to

$$w_k = (\bar{\mu}_k{}^H - \bar{\mu}_k{}^B + g_k) - \left[\frac{kT}{N_k}\right] \ln \phi_k + \frac{1}{6}\sum_{k'} B_{kk'}\nabla^2 c_{k'} - \frac{\nu_k}{6\nu_s}\sum_{k'} B_{sk'}\nabla^2 c_{k'} \qquad (3.12)$$

where $\bar{\mu}_k$ are exchange chemical potentials defined by

$$\bar{\mu}_k \equiv \mu_k - \frac{\nu_k}{\nu_s}\mu_s = \nu_k \frac{\partial \tilde{F}}{\partial \phi_k} \tag{3.13}$$

For complete equilibrium of a single homopolymer–solvent mixture, eq 3.11 and 3.12 define the relative pressure and optimal mean field for the polymer as

$$(p_B - p) = \frac{(\mu_s^H - \mu_s^B)}{\nu_s} + \frac{kT(\chi s^2)}{6\nu_p}\nabla^2\phi_p$$

$$\omega_p = (\bar{\mu}_p^H - \bar{\mu}_p^B) - \left(\frac{kT}{N_p}\right)\ln \phi_p - \frac{kT(\chi s^2)}{3}\nabla^2\phi_p \tag{3.14}$$

where $B_{sp} \equiv kT(\chi s^2)\nu_s$ in terms of the Flory interaction parameter χ and a coefficient s^2 which is on the order of the square of the segment length a_p. The optimal mean field in eq 3.14 is used with eq 2.3 and 2.4 to give

$$\frac{1}{N_p}\frac{\partial q_p}{\partial \tau} = \frac{a_p^2}{6}\nabla^2 q_p - \left(\frac{w_p}{kT}\right)q_p$$

$$\phi_p(\vec{x}) = \int_0^1 d\tau\, q_p(\vec{x},\tau)\, q_p(\vec{x},1-\tau) \tag{3.15}$$

which predicts the value of the polymer volume fraction $\phi_p(\vec{x})$ at a local position $\vec{x}$. In the limit of very large polymer index or for concentrated solutions in good solvents, where long-range correlations are screened by excluded volume interactions, the function q_p can be regarded as independent of τ, and eq 3.15 reduce to

$$\nabla^2 q_p - \left(\frac{6w_p}{kTa_p^2}\right)q_p \cong 0$$

$$\phi_p(\vec{x}) \cong q_p^2(\vec{x}) \tag{3.16}$$

These relations and eq 3.14 will be used later in the analysis of depletion forces that cause attraction between surfaces in aqueous solutions of large nonadsorbent polymers and good solvent conditions. (With the exception of the Lagrange multipliers for the restricted exchange constraints, eq 3.10–3.16 are those derived by Hong and Noolandi.)[4]

IV. Mechanical Work To Displace Surfaces of Fixed Area or To Increase Gap Area at Constant Separation

The mechanical work to increase the separation z_g at constant surface area defines the force per unit area on each surface, a normal stress σ_p

$$\delta W|_A = (\sigma_p A)\delta z_g \tag{4.1}$$

(Stress is defined as positive in the sense of the normal to the surface; i.e., positive stress is attractive, and negative stress is repulsive.) Similarly, the mechanical work to enlarge the interfacial area of the surfaces at constant separation defines an interfacial tension γ

$$\delta W|_{z_g} = \gamma \delta A \tag{4.2}$$

The mechanical work per displacement is given explicitly in continuum mechanics as the integral of the stress field multiplied by the rate at which deformation increases with displacement.[5] This is usually given as a work per unit time increment or mechanical power

$$\frac{\delta W}{\delta t} = \int (\sum_{\alpha\beta}\sigma_{\alpha\beta}V_{\alpha\beta})\, d^3x \tag{4.3}$$

where t is time and $\sigma_{\alpha\beta}$ is the Eulerian stress tensor and $V_{\alpha\beta}$ is the instantaneous rate of deformation tensor. For isotropic stress $(p_B - p)$ and a deviatoric stress $\tilde{\sigma}$, the contracted product of these tensors is simply

$$\sum_{\alpha\beta}\sigma_{\alpha\beta}V_{\alpha\beta} \equiv (p_B - p)\frac{\partial \ln \lambda}{\partial t} + \tilde{\sigma}\frac{\partial \ln \tilde{\lambda}}{\partial t}$$

where $\tilde{\lambda}$ is the deformation variable that represents elongation or compression at *constant volume*, i.e., the aspect ratio of length divided by the square root of the cross section. [For axisymmetric geometries, the stress field is defined by axial (aligned along the coordinate normal to the surfaces) and lateral (parallel to the surfaces) stresses given by principal stresses σ_z and σ_α, as shown in the Appendix. In turn, the prinicipal stresses can be separated into isotropic (mean) and deviatoric (shear) contributions, i.e., $\sigma_z \equiv \sigma_0 + \tilde{\sigma}$ and $\sigma_\alpha \equiv \sigma_0 - \tilde{\sigma}/2$.] Hence, the general relation for increment in mechanical work with displacement is

$$\delta W = \int [(p_B - p)\delta\lambda]\, d^3x_0 + \int \tilde{\sigma}[\lambda_\alpha \delta\lambda_z - (\lambda_z/2)\delta\lambda_\alpha]\, d^3x_0 \tag{4.4}$$

when expressed in terms of the reference coordinates d^3x_0. The deviatoric deformation (shear) at constant volume has been expressed in terms of coordinate dilation ratios (λ_z, λ_α), which are defined appropriate to the planar geometry:

$$\lambda_z \equiv dz/dz_0; \qquad \lambda_\alpha \equiv A/A_0; \qquad \lambda_z\lambda_\alpha \equiv \lambda$$

Equation 4.4 can also be written as

$$\delta W = \int \delta[(p_B - p)\lambda]\, d^3x_0 + \int (\lambda \delta p)\, d^3x_0 + \int \delta(\tilde{\sigma}\lambda/2)\, d^3x_0 + \int [(\lambda_\alpha/2)\delta(\tilde{\sigma}\lambda_z) - \lambda_z\delta(\tilde{\sigma}\lambda_\alpha)]\, d^3x_0$$

and more usefully as

$$\delta W = \delta \int \left[(p_B - p) + \frac{\tilde{\sigma}}{2}\right] d^3x + \int \left[\delta p + \frac{\delta(\tilde{\sigma}\lambda_z)}{2\lambda_z} - \frac{\delta(\tilde{\sigma}\lambda_\alpha)}{\lambda_\alpha}\right] d^3x \tag{4.5}$$

in terms of "instantaneous" coordinates d^3x.

The force per unit area on the surfaces is obtained with eq 4.1 and 4.5 as

$$\sigma_p = \frac{\delta}{\delta z_g}\left(\int_0^{z_g}[(p_B - p) + \tilde{\sigma}]\, dz\right) + \int_0^{z_g}\left(\frac{\delta p}{\delta z_g} - \frac{\delta \tilde{\sigma}}{\delta z_g}\right) dz \tag{4.6}$$

where it is assumed that the stress field depends only on the distance z from a surface (with no lateral dependence). For symmetric polymer–surface interactions, eq 4.6 reduces to a simple result

$$\sigma_p = p_B - p_h + \tilde{\sigma}_h \tag{4.7}$$

where $p_h = p(z=h)$, $\tilde{\sigma}_h = \tilde{\sigma}(z=h)$, and $h = z_g/2$. The force per unit area on each plate is just the stress evaluated at the midpoint of the gap!

The interfacial tension can be derived from eq 4.2 and 4.5 as

$$\gamma = \frac{\delta}{\delta A}\left(A\int_0^z\left[(p_B - p) - \frac{\tilde{\sigma}}{2}\right] dz\right) + A\int_0^{z_g}\left(\frac{\delta p}{\delta A} + \frac{1}{2}\frac{\delta \tilde{\sigma}}{\delta A}\right) dz$$

or

$$\gamma = \int_0^{z_g}\left[(p_B - p) - \frac{\tilde{\sigma}}{2}\right] dz \qquad (4.8)$$

where edge effects at the entrance to the gap adjacent to the bulk solution have been ignored. Edge effects enter as steep lateral stress gradients proximal to the gap entrance. Such contributions scale as the gap perimeter divided by the gap area and are thus usually negligible.

The mean-field representation for the deviatoric stress can be deduced from the equivalence between interfacial tension and the excess free energy of the gap per unit area. The free energy per unit area of the gap is given by

$$\frac{F}{A} = \int_0^{z_g}\sum_k c_k\left[\mu_k^H - \left(w_k + \frac{kT}{N_k}\ln\phi_k\right) + \frac{1}{12}\sum_{k'}B_{kk'}\nabla^2 c_{k'}\right] dz$$

Thus, the excess free energy per unit area is obtained as

$$\frac{1}{A}(F - \sum_k n_k\mu_k^B) = \int_0^{z_g}\left[(p_B - p) - \sum_k c_k\left(g_k + \frac{1}{12}\sum_{k'}B_{kk'}\nabla^2 c_{k'}\right)\right] dz$$

which is the result derived in earlier references[4] and must equal the interfacial tension. Hence, the deviatoric stress is

$$\tilde{\sigma} = 2\sum_k c_k\left(g_k + \frac{1}{12}\sum_{k'}B_{kk'}\nabla^2 c_{k'}\right)$$

With the equation for isotropic stress given by eq 3.11 the force per unit area on each surface plus the interfacial tension are established as

$$\sigma_p = \frac{1}{\nu_s}\left(\mu_s^H - \mu_s^B + \frac{1}{6}\sum_{k'}B_{sk'}\nabla^2 c_{k'}\right)\Big|_{z=h} + 2\sum_k c_k\left(g_k + \frac{1}{12}\sum_{k'}B_{kk'}\nabla^2 c_{k'}\right)\Big|_{z=h} \qquad (4.9)$$

$$\gamma = \frac{1}{\nu_s}\int_0^{z_g}\left(\mu_s^H - \mu_s^B + \frac{1}{6}\sum_{k'}B_{sk'}\nabla^2 c_{k'}\right) d^3z - \sum_k\int_0^{z_g} c_k\left(g_k + \frac{1}{12}\sum_{k'}B_{kk'}\nabla^2 c_{k'}\right) dz \qquad (4.10)$$

Clearly, the primary source for the deviatoric stress is restricted exchange of polymer chains explicitly represented by the Lagrange multipliers g_k; additional contributions come from nonlocal effects. In the sections to follow, nonlocal terms will be neglected, and the chains will be assumed to be in complete equilibrium with the bulk solution. Thus, the force per unit area on the surfaces and interfacial tension depend only on the local relative osmotic pressure in the solution, i.e.

$$\sigma_p = \Pi_B - \Pi_h$$

$$\gamma = \int_0^{z_g}(\Pi_B - \Pi)\, dz \qquad (4.11)$$

since osmotic pressure is given by the chemical potential of the solvent divided by the volume per solvent molecule, $\Pi_B - \Pi(z) \equiv (\mu_s^H - \mu_s^B)/\nu_s$.[8]

The above result for interfacial free energy density (tension) as the integral of the osmotic pressure over the gap region was originally obtained by Joanny, Leibler, and de Gennes[3] for the limit of infinite polymer index to represent depletion effects in semidilute solutions with good solvent conditions. Likewise, Scheutjens and Fleer[2] concluded that the interfacial free energy density for depletion was of the same form on the basis of a lattice mean-field approach. However, in previous developments, the force per unit area on surfaces has always been inferred from the derivative of the interfacial free energy density with respect to separation z_g

$$\frac{\delta}{\delta z_g}[\gamma(z_g) - 2\gamma(\infty)] = \sigma_p - \int_0^{z_g}\frac{\delta\Pi}{\delta z_g} dz \qquad (4.12)$$

which clearly differs from the surface stress. The work potential $\tilde{W}$ (energy per unit area) required to assemble the surfaces from large separation ($-\infty$) to a specific gap dimension is the integral of the force per unit area over the full range of displacement

$$\tilde{W} \equiv \int_\infty^{z_g}\sigma_p\, dz_g' = -\int_{z_g}^\infty \sigma_p\, dz_g' \qquad (4.13)$$

As will be demonstrated, the interaction potential $\tilde{W}$ given in eq 4.13 does not have the same dependence on separation as the interfacial tension (relative to two surfaces at infinite separation).

V. Depletion Forces in Semidilute Solutions and Good Solvent Conditions

In good solvent conditions and semidilute concentrations, the large molecular weight approximation is appropriate and leads to eq 3.16 as prediction of the inhomogeneous polymer distribution:

$$\nabla^2 q - \left(\frac{6w_p}{kTa_p^2}\right)q \cong 0$$

$$q^2 = \nu_p c_p \equiv \phi$$

$$1 - q^2 = \nu_s c_s = 1 - \phi \qquad (5.1)$$

Here, the optimal mean field w_p is given by eq 3.14 in terms of the local exchange chemical potential as

$$w_p = \bar{\mu}_p^H - \bar{\mu}_p^B$$

Complete equilibrium is assumed, and nonlocal effects are neglected. By use of Flory theory[8] to represent chemical potentials, the large molecular weight limit leads to the following approximation for a semidilute range of concentrations

$$\frac{(\bar{\mu}_p^H - \bar{\mu}_p^B)}{kT\nu_s} \cong \frac{(1-2\chi)\phi_B}{\nu_s}\left(1 - \frac{\phi}{\phi_B}\right)$$

$$\frac{(\mu_s^H - \bar{\mu}_s^B)}{kT\nu_s} \cong \frac{(1-2\chi)\phi_B^2}{2\nu_s}\left[1 - \left(\frac{\phi}{\phi_B}\right)^2\right]$$

where ϕ is the local volume fraction of polymer and χ is the Flory parameter that characterizes the quality of the solvent ($\chi < 0.5$ represents good solvents). The length scale ξ for correlations is obtained from the coefficient of the optimal mean field in eq 5.1

$$\xi^2\nabla^2 q + \left(1 - \frac{q^2}{\phi_B}\right)q \simeq 0$$

$$\xi \equiv a_p\left(\frac{\nu_s}{6\nu_p(1-2\chi)\phi_B}\right)^{1/2} \qquad (5.2)$$

in proportion to the statistical segment length a_p of the

polymer. The correlation length is used to scale eq 5.1 to dimensionless (universal) form.

Integration of the one-dimensional approximation for parallel surfaces yields

$$\xi^2\left|\frac{d\phi}{dz}\right|^2 = 4\phi(\phi_h - \phi)[1 - (\phi_h + \phi)/2\phi_B] \qquad (5.3)$$

Final integration of eq 5.3 leads to a transcendental relation for the volume fraction at a local position z; ϕ_h and ϕ_B are volume fractions at the midpoint of the gap and in the reference solution, repectively.

With the volume fraction profiles predicted by eq 5.3 and with eq 4.11 and 4.12, universal curves are obtained for the depletion stress and for the derivative of the interfacial tension with respect to separation as shown in Figure 1a. Because of the reduced osmotic pressure in the gap, depletion forces are attractive and draw the surfaces together. The stress units in Figure 1 have been scaled by the osmotic pressure of the reference solution. It is apparent that the depletion stress decays much more slowly than the derivative of the interfacial tension as the surfaces are separated. This is very important since the slower decay implies a much longer effective range of attraction between the surfaces. The depletion stress can be integrated from large separation to specific distances to give the interaction potential; this result is compared with the interfacial tension (relative to two surfaces at infinite separation) as a function of separation in Figure 1b. Here, energies per unit area are scaled by the product of reference solution osmotic pressure and the correlation length. In Figure 1, separation distances are scaled by the correlation length defined by eq 5.2. In Figure 1b, the interaction potential is larger than the interfacial free energy density at any gap separation because of the longer range action of the mechanical stress.

VI. Direct Measurements of Interaction Potential in Concentrated Solutions of Nonadsorbent Polymers

Until recently, measurement of attractive forces between surfaces due to polymer depletion have not been accessible to direct experiment. This is because the forces are very small in dilute solutions and are masked by other forces such as polymer bridging. Likewise, difficulties associated with measurement in concentrated polymer solutions have inhibited tests at higher volume fractions. In order to quantitate weak attraction between molecularly smooth surfaces (roughness scale $< 10^{-7}$ cm), we developed a simple method based on controlled adhesion of surfactant bilayer membranes made from diacyl lipid molecules. In this approach (see ref 6 and 10), bilayer membranes are formed as vesicular capsules (about 10^{-3} cm in diameter). The choice of diacyl lipids leads to vesicles that deform as closed surfaces with essentially constant local surface density and constant trapped volume. The capsules are initially formed in a slightly deflated state relative to a perfect sphere, which leaves the bilayer membrane completely flaccid. Hence, the vesicle offers no resistance to deformation until pressurized into a spherical form. To measure adhesion energies, two vesicles are aspirated into separate suction micropipets, which they enter with negligible suction pressure until the portions of the vesicles outside the pipets are pressurized into spherical segments. Further displacement into the pipets is negligible as the pressure is increased, but bilayer tensions increase in direct proportion to the applied suction pressures. These vesicles are then maneuvered into close proximity to permit adhesion. One vesicle is held with high suction pressure that

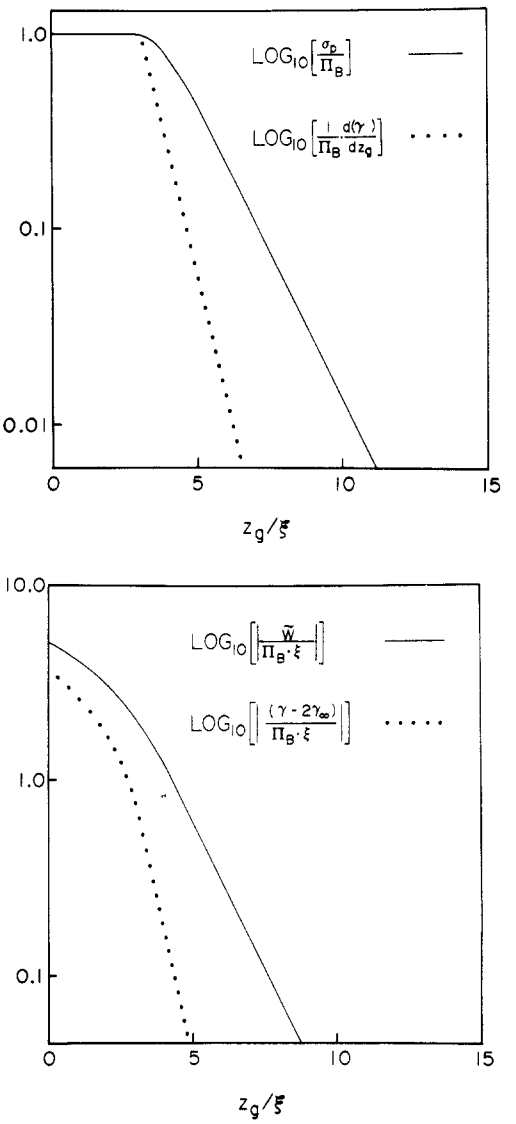

Figure 1. Predictions of depletion force per unit area, interaction (work) potential, and interfacial free energy (tension) per unit area for a solution of nonadsorbent polymers confined between rigid surfaces as derived from self-consistent field analysis for different surface separations. The gap solution was assumed to be in complete equilibrium with a bulk solution at semidilute concentration and in good solvent conditions. (a, Top) Logarithms of the stress on the surfaces given by the osmotic pressure reduction at the midpoint of the gap *and* the derivative of the interfacial tension with respect to gap dimension (both normalized by osmotic pressure of the bulk solution) plotted versus separation normalized by the characteristic length ξ for correlations. (b, Bottom) Logarithms of the magnitudes of the interaction potential (work per unit area to assemble surfaces from large separation) *and* the interfacial tension relative to infinite separation (both normalized by the product of osmotic pressure in the bulk solution and the length scale ξ) plotted versus dimensionless separation between the surfaces.

creates a large membrane tension (order of a few dynes per centimeter), which keeps the vesicle surface shaped as a stiff spherical segment. The second vesicle (called the "adherent" vesicle) is held with a very low suction pressure sufficient to initially maintain a spherical contour. This vesicle is positioned to just touch the stiff spherical vesicle surface at a single point. Then the suction pressure is reduced, which allows the membrane to spread onto the stiff spherical vesicle surface. The suction applied to the adherent vesicle is reduced by discrete steps, and the equilibrium geometry at each step is observed (an example is shown in Figure 2). Next, the suction is increased by similar steps to separate the adherent vesicle from the

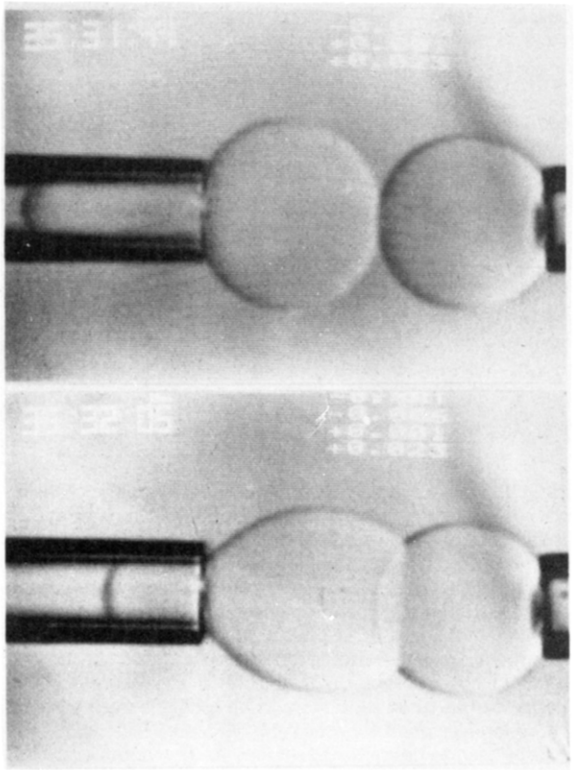

Figure 2. Video micrograph of the equilibrium adhesion configuration formed by allowing one vesicle lipid bilayer to spread on a second vesicle surface (which was pressurized into a stiff spherical contour). The tension in the adherent vesicle bilayer (left side) was controlled to limit the spreading and yielded the adhesion energy per unit area (0.12 erg/cm^2 in the concentrated dextran polymer solution at volume fraction of 0.057). Tensions and the extent of coverage by the adherent vesicle were controlled by pipet suction pressures. Pipet caliber $\simeq 5 \times 10^{-4}$ cm; vesicle diameters $\simeq 20 \times 10^{-4}$ cm.

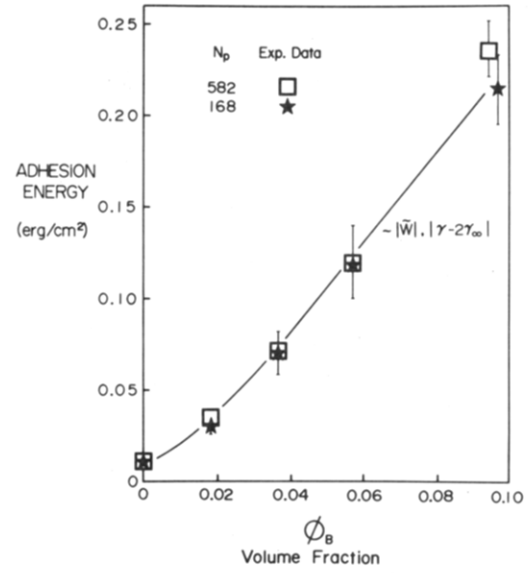

Figure 3. Direct measurements of adhesion energy per unit area for assembly of electrically neutral phosphatidylcholine bilayer membranes in aqueous solutions of nonadsorbent polymers (dextran) over volume fractions from 0.0 to 0.1. Osmotic pressures of these solutions yielded a Flory interaction parameter of 0.428—characteristic of good solvent conditions.[6] With this parameter, the interaction potential and interfacial free energy (per unit area) were predicted, including the small "background" attraction due to van der Waals forces between the bilayers.[6,10] The only undetermined parameter was the statistical segment length; values were chosen separately for each energy measure to give the same correlation with the adhesion energies shown by the solid line: $a_p = 6.2 \times 10^{-8}$ cm for the interaction potential and $a_p = 8.5 \times 10^{-8}$ cm for the interfacial free energy density. Data taken from ref 6.

spherical test surface. Thus, reversibility of the adhesive contact is established. From analysis of mechanical equilibrium of the adherent configurations, the experimental measurements (suction pressure *versus* fractional area of the spherical surface covered by the adherent membrane) are converted to membrane tension *versus* the macroscopic contact angle θ_c between the vesicle membranes. The tension correlates with a constant divided by $1 - \cos \theta_c$ for both adhesion and separation processes. Thus, this constant is the reversible work (free energy) associated with formation of a unit area of adhesive contact. Since membrane regions are initially separated by macroscopic dimensions ($\sim 10^{-4}$ cm) and subsequently form stable contact with separations on the order of 10^{-7} cm, the work to form a unit area of contact is the interaction potential defined by eq 4.13, where z_g is the final gap dimension.

The procedure outlined above has been used to measure interaction potentials for the intrinsic colloidal attraction (net potential of van der Waals attraction minus hydration and electric double-layer replusion) between bilayer membranes made from various diacyl lipids in aqueous buffers.[10] Likewise, the much stronger attraction induced by nonadsorbent polymers (poly(glucose)–dextran and poly(ethylene oxide)) has also been measured with this technique.[6,11] Depletion was verified directly by evaluating the amount of fluorescently labeled polymer present in the contact region between adherent vesicle pairs.[6] For electrically neutral vesicle surfaces, no polymer was detectable in the contact region, which implied that the concentration in the gap between membranes was reduced to less than 10% of the bulk concentration (based on the limit of experimental resolution). Consistent with the semidilute range of concentrations, the measured values of interaction potential showed no dependence on molecular weight. Further, it was shown that the interaction potential predicted by eq 4.13 and 5.3 correlated extremely well with the measured values for adhesion of electrically neutral bilayers over a wide range of voume fraction (0.01–0.1).[6] All parameters in the SCF prediction of the inteaction potential were determined by independent measurements a priori (e.g., Flory interaction parameter, volume fraction, molecular weights and densities) *except* the statistical segment length a_p. Since the statistical segment length is chosen once to give the best fit to *all* experiments with the same polymer for several molecular weights and volume fractions, the test of the theory is reasonably stringent. However, both the interaction potential (eq 4.13) and the interfacial free energy density of the gap relative to infinite separation (eq 4.11) scale as the product of the reference solution osmotic pressure and the correlation length ξ, i.e., as volume fraction to the 3/2 power. As is apparent in Figure 1b, the difference between these two measures of energy is about 60% when the surfaces are at close contact. This difference can be nullified by choosing different statistical segment lengths. For example, Figure 3 shows results for adhesion energies measured with neutral vesicles in dextran solutions correlated with the relations for both interaction potential $\tilde{W}$ and interfacial free energy density $\gamma - 2\gamma_\infty$. Two different statistical segment lengths were required: $a_p = 6.2$ Å for the interaction potential defined by eq 4.13 and $a_p = 8.5$ Å for the interfacial free energy density relation defined by eq 4.11. Even though the values for interaction potential and interfacial free energy density can be made the same by appropriate choice of

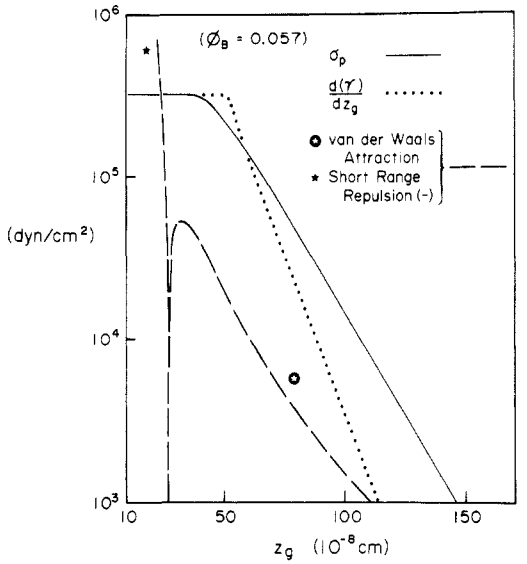

Figure 4. Depletion force (per unit area) and the rate of change of the interfacial free energy density with respect to separation *predicted* for a specific concentration (9.3% wt/vol ≡ 0.057 volume fraction) of nonadsorbent dextran polymer. The statistical segment lengths used to calculate each stress measure were the same values as for Figure 3, chosen to yield equivalent values for the interaction potential and interfacial free energy density at final contact, i.e., 0.12 erg/cm² for ϕ_B = 0.057. Also shown are the magnitudes of the weak "background" attraction due to long-range van der Waals forces and the stiff repulsion (–) at close range from hydration forces; the latter establishes the final separation distance (~24 × 10^{-8} cm).[6,10]

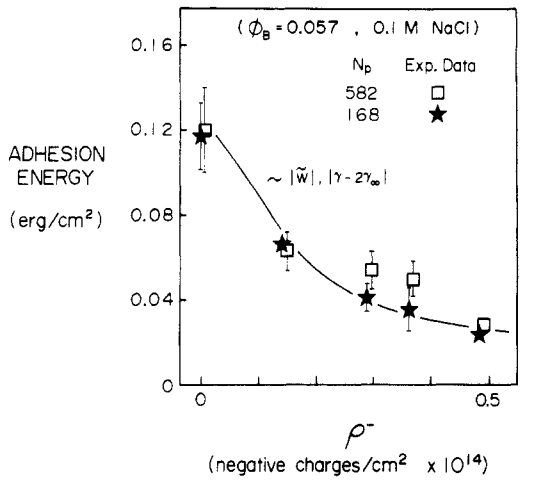

Figure 5. Direct measurements of adhesion energy per unit area for assembly of electrically charged phospholipid bilayer membranes in aqueous solutions of nonadsorbent polymers (dextran) at fixed volume fraction (ϕ_B = 0.057) plus 0.1 M NaCl. Surface charge density was derived from the mole fraction of negatively charged surfactant (phosphatidylserine (PS)), which was mixed with the neutral lipid (phosphatidylcholine (PC)) in the bilayers.[6] Also shown are predictions for attenuation of the interaction potential and interfacial free energy (per unit area) caused by electric double-layer repulsion. The Debye length for decay of the double-layer repulsion was 9.6 × 10^{-8} cm. The attractive stress measures used to predict the energies are shown in Figure 4. Data taken from ref 6.

segment length, the distance dependences of the force measures calculated from derivatives of each function with respect to separation are significantly different. For example, Figure 4 shows the two derivatives versus separation calculated for a specific dextran concentration (9.3% wt/vol ≡ 0.057 volume fraction) where the depletion-induced attraction was 1 order of magnitude greater than the intrinsic van der Waals attraction between the neutral lipid bilayers. Also plotted in Figure 4 is the weak "background" attraction due to long-range van der Waals forces and the stiff repulsion at close range from hydration forces, which establishes the final separation distance.[6,10] Clearly, the critical test was to evaluate the distance dependence of the attractive potential.[12]

In order to test the dependence of attraction on separation, fixed electric charges were added to the surfaces to create repulsive stresses that would enlarge the separation between surfaces. It is well established that electric double-layer repulsion in monovalent salts can be predicted by classical theory and behaves as an exponentially decaying field when separation distances exceed the characteristic decay length (Debye length).[10,13] By choosing ionic strengths to give Debye lengths that closely bracketed the decay length for depletion, we could predict different dependencies on the surface charge density for the interaction potential and interfacial free energy density. Figure 5 shows the attenuation of adhesion energy measured for negatively charged vesicles in 0.1 M NaCl–dextran polymer solutions at fixed volume fraction of ϕ_B = 0.057. Here, the Debye length for decay of the double-layer repulsion in 0.1 M NaCl was calculated to 9.6 × 10^{-8} cm. The vesicles were preformed from mixtures of phosphatidylserine with a single negative charge and neutral phosphatidylcholine lipids. Also shown in Figure 5 are predictions for attenuation of the interaction potential and interfacial free energy density produced by electric double-layer forces; the energy measures begin at zero surface charge density with values for adhesion of electrically neutral surfaces. Repulsive stresses were calculated by using double-layer theory[14] and published values for lipid surface densities derived from X-ray diffraction studies. The attractive stresses were the same as those shown in Figure 4 for neutral bilayer interactions. For 0.1 M NaCl and a Debye length of 9. 6 Å, both energy measures correlated well with the observed attenuation of adhesion energy as surface charge density was increased, because both depletion length scales were longer than the Debye length. Therefore, adhesion energies were tested in solutions fixed at the same dextran concentration but with lower ionic strength (0.023 M NaCl). Here, the Debye length was calculated to be twice the value for 0.1 M NaCl, i.e., 20 Å. Figure 6 presents the measurements of attenuation of adhesion energy and predictions for interaction potential and interfacial free energy density plotted as functions of surface charge density. There is a clear difference between the attenuation of interaction potential and interfacial free energy density. The interfacial free energy density predicts an abrupt "unbinding" transition whereas the interaction potential exhibits a continuous energy attenuation until low levels of adhesion strength are reached consistent with the measured values of adhesion energy. At this lower ionic strength, the weak van der Waals attraction between the bilayers plays a significant role because it overcomes the electric double-layer repulsion at large separations (>200 Å) to bring the surfaces into the range of the depletion force (which decays more rapidly at very large distances than the double-layer force, as illustrated in Figure 4).

Conclusions

The self-consistent field theory for an incompressible polymer solution confined between parallel surfaces predicts the existence of a nonuniform hydrostatic pressure field relative to the uniform bulk pressure. This field is given by the local osmotic pressure difference relative to the bulk solution in the absence of nonlocal effects. Further, the incremental work to displace surfaces of

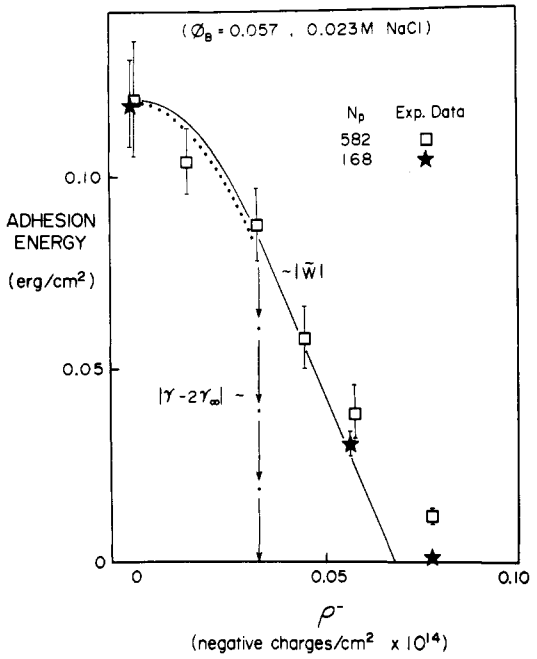

Figure 6. Direct measurements of adhesion energy per unit area for assembly of electrically charged phospholipid bilayer membranes in aqueous solutions of a nonadsorbent polymer (dextran) at fixed volume fraction (ϕ_B = 0.057) plus 0.023 M NaCl. Surface charge density was derived from the mole fraction of negatively charged surfactant (phosphatidylserine (PS)), which was mixed with the neutral lipid (phosphatidylcholine (PC)), in the bilayers. Also shown are predictions for attenuation of the interaction potential and interfacial free energies (per unit area) caused by the electric double-layer repulsion. The Debye length for decay of the double-layer repulsion was 20 × 10^{-8} cm. As for Figure 5, the energies were calculated with the attractive stresses plotted in Figure 4. Note the fivefold expansion of the charge density scale.

constant area is simply given by the axial mean-field stress at the *center* of the gap × incremental displacement. The axial stress is the sum of the relative hydrostatic pressure plus a deviatoric stress component derived primarily from restricted exchange effects. For complete equilibrium, the interaction potential is the integral of the relative pressure at the center of the gap over seprations from infinity to final contact. As was shown in the text, the interaction potential differs from the interfacial free energy density of the gap (relative to infinite separation). The difference between these two measures of energy is the rate of change of the hydrostatic field with respect to separation cumulated over the gap volume. This difference is analogous to the comparison of a work potential and a Gibbs potential; i.e., the $V\mathrm{d}P$ term must be extracted from the differential of the Gibbs energy to obtain the differential of the work potential. The important result is that the force per unit area on the surfaces (physical stress) is given by the relative osmotic pressure at the center of the gap, which exhibits a longer range action than the derivative of the interfacial free energy density with respect to separation. Obviously, at complete equilibrium interaction between the surfaces is driven exclusively by relative activity of the solvent. This result is the same for both absorbent and nonadsorbent polymers. However, restricted exchange of polymers between the gap and bulk regions can greatly affect the force on the surfaces both by increasing the concentration of segments at the center of the gap (thereby raising the relative osmotic pressure at the center) and by creating deviatoric stress through constraint forces.

Tests of adhesion between lipid bilayer membranes of vesicles have been used to directly quantitate the interaction potential for assembly of surfaces in aqueous media from large (infinite) separation to intimate contact. By use of this approach in concentrated solutions of nonadsorbent polymers, depletion energies were measured and compared with predicted values for both interaction potential and interfacial free energies (per unit area). In these comparisons, the only undetermined parameter was the statistical segment length. For electrically neutral surfaces, appropriate choice of segment length could yield excellent correlation between measured adhesion energies and either energy potential, but the value of the segment length required for the interfacial free energy density weas about 40% greater than the value for the interaction potential. On the other hand, measurements of adhesion with electrically charged surfaces in different ionic strength solutions provided a critical test of the distance dependence of the adhesion energy. The results correlated with the slower decay predicted for the interaction potential even though the segment length chosen for the interfacial free energy density was much larger.

Unlike the depletion case, adsorption is much more complicated because of chain bridging and restricted equilibrium conditions. These effects have been observed and quantitated in dilute polymer solutions by elegant direct force measurements.[15] Likewise, similar model cases have been analyzed by Scheutjens and Fleer[2] with lattice mean-field methods to predict segment distributions, bridging chain fractions, interfacial free energy densities, etc. With calculations of segment distributions and bridging chain fractions, plus auxiliary specification of exchange properties between gap and bulk regions, the relative contribution of deviatoric versus isotropic stress (hydrostatic pressure) to the total axial stress can be estimated and compared with the direct force measurements to further test mean-field predictions.

Acknowledgment. This work was supported in part by the National Institutes of Health, Grant GM38331, and the Canadian MRC, Grant MT7477. I gratefully acknowledge the expert technical assistance of V. Rawicz, who carried out the recent vesicle adhesion tests in low ionic strength solutions.

Appendix

The principal stresses (σ_z, σ_α), which act on a domain element (d^3x), are illustrated below for the assumption of axial symmetry.

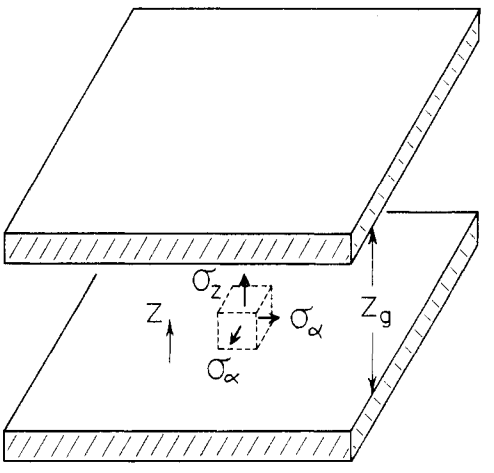

Likewise, the principal deformation ratios (λ_z, λ_α), which represent geometric extension of the reference domain

(d^3x_0) when the surfaces are displaced, are defined as shown in the following sketch:

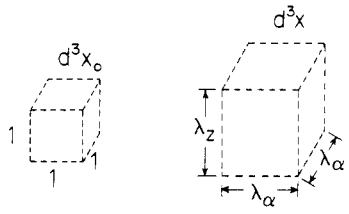

Registry No. Dextran, 9004-54-0.

References and Notes

(1) Mackor, E.; van der Waals, J. *J. Colloid Sci.* **1952**, *7*, 535.
(2) Roe, R. J. *J. Chem. Phys.* **1974**, *60*, 4192. Scheutjens, J. M. H. M.; Fleer, G. F. *Adv. Colloid Interface Sci.* **1982**, *16*, 361; **1983**, *18*, 309. Scheutjens, J. M. H. M.; Fleer, G. F. *Macromolecules* **1985**, *18*, 1882.
(3) Edwards, S. F. *Proc. Phys. Soc., London* **1965**, *85*, 613. de Gennes, P. G. *Rep. Prog. Phys.* **1969**, *32*, 187. Joanny, J. F.; Leibler, L.; de Gennes, P. G. *J. Polym. Sci., Polym. Phys. Ed.* **1979**, *17*, 1073. de Gennes, P. G. *Macromolecules* **1982**, *15*, 492.
(4) Helfand, E. *J. Chem. Phys.* **1975**, *62*, 999. Helfand, E.; Sapse, A. M. *J. Chem. Phys.* **1975**, *62*, 1327. Helfand, E.; Sapse, A. M. *J. Polym. Sci., Polym. Symp.* **1976**, *No. 54*, 289. Hong, K. M.; Noolandi, J. *Macromolecules* **1981**, *14*, 727.
(5) Prager, W. *Introduction to the Mechanics of Continua*; Dover: New York, 1961.
(6) Evans, E.; Needham, D. *Macromolecules* **1988**, *21*, 1822.
(7) Cahn, J. W.; Hilliard, J. E. *J. Chem. Phys.* **1958**, *28*, 258.
(8) Flory, P. J. *Principles of Polymer Chemistry*; Cornell University Press: Ithaca, NY, 1953.
(9) The nature of chemical interaction between polymer segments and the surfaces (i.e., "adsorption" or "nonadsorption" behavior) is represented by a short-range potential cumulated into a contact energy per unit area based on segment concentrations proximal to the surfaces. For weak segment binding, local equilibrium near the surface implies that the contact energy per unit area is proportional to the gradient of segment concentration and thus establishes an effective boundary condition for the continuous segment distributions away from the surfaces.[4,7] Hence, no explicit term for the contact energy appears in the free energy functional. When segment binding to the surface is very strong, then nonequilibrium effects will be important. In the extreme, the boundary condition takes the form of "grafted" chains of various lengths and loops, which will be reflected in the probability distributions $q_k(\vec{x},\tau)$.
(10) Evans, E.; Needham, D. *J. Phys. Chem.* **1987**, *91*, 4219.
(11) Evans, E.; Needham, D. In *Molecular Basis of Membrane Fusion*; Ohki, S., Doyle, D., Flanagan, T. D., Hui, S. K., Mayhew, E., Eds.; Plenum Press: New York, 1988; p 83.
(12) Predictions of depletion forces and energies for the dextran polymer solutions were calculated with a value of $\chi = 0.428$ measured for the Flory interaction parameter by osmometry; solutions were made with polymers of various molecular weights (in the range of MW 10 000–200 000). No significant dependence on molecular weight was observed. The volume fractions of the solutions were determined by polarimetry.[6]
(13) Israelachvili, J. N.; Pashley, R. M. in *Biophysics of Water*; Franks, F., Ed.; Wiley: New York, 1982; p 183. Marra, J.; Israelachvili, J. *Biochemistry* **1985**, *24*, 423.
(14) Verwey, E. J. W.; Overbeek, J. Th. G. *Theory of the Stability of Lyophobic Colloids*; Elsevier: Amsterdam, 1948.
(15) Klein, J. *J. Chem. Soc., Faraday Trans. 1* **1983**, *79*, 99. Klein, J.; Luckham, P. F. *Nature* **1984**, *308*, 836. Luckham, P. F.; Klein, J. *Macromolecules* **1985**, *18*, 721. Klein, J. *J. Colloid Interface Sci.* **1986**, *111*, 305. Marra, J.; Hair, M. *Macromolecules* **1988**, *21*, 2349. Marra, J.; Hair, M. *Macromolecules* 1988, *21*, 2356.

Phase Diagram of Aqueous Solutions of (Hydroxypropyl)cellulose

Suzie Fortin and Gérard Charlet*

Centre de Recherches en Sciences et Ingénierie des Macromolécules (CERSIM) and Department of Chemistry, Université Laval, Cité Universitaire, Quebec, Canada, G1K 7P4.
Received August 16, 1988; Revised Manuscript Received October 25, 1988

ABSTRACT: The phase diagram of aqueous solutions of (hydroxypropyl)cellulose has been determined for carefully fractionated samples having a degree of substitution between 2.8 and 3.0, a molar substitution between 5.8 and 6.3, and a molecular weight between 28 and 140 kg·mol^{-1}. The diagram is composed of three regions. Isotropic solutions are stable below 42 °C at polymer weight fractions lower than about 50%. Cholesteric liquid crystals are formed at concentration higher than 55% and phase separate at a lower temperature than isotropic solutions. The difference may be as large as 28 deg for the lowest molecular weight sample. At high temperature, only concentrated mesophases are homogeneous. All other compositions consist of a cholesteric phase and an infinitely dilute solution. A single biphasic region, whose width depends on temperature, extends over the whole water normal liquid range. Phase separation is responsible for unusual optical properties of some anisotropic solutions, including a negative temperature dependence of the cholesteric pitch.

Introduction

(Hydroxypropyl)cellulose (HPC) is a water-soluble cellulose derivative. It is usually synthesized by the reaction of propylene oxide on cellulose under alkaline conditions, giving lateral chains containing a variable number of hydroxypropoxy groups. Commercial samples having[1] a degree of substitution DS (i.e., the average number of oxygen of the original cellulose repeat unit bearing a substituent) above 2.8 and a molar substitution, MS (i.e., the average number of hydroxypropyl substituent per anhydroglucose residue), larger than 4 have been widely studied. Numerous properties of the polymer in dilute aqueous solutions have been examined, including phase separation,[1,2] configurational parameters,[3,4] conformation,[5] surface tension,[6] or adsorption behavior.[7] Concentrated solutions of HPC in a variety of aqueous and organic solvents form liquid crystals. The occurrence of an ordered phase is observed for most soluble cellulosic polymers[8,9] and is presumably related to the lack of flexibility of the cellulose backbone. The chirality of the anhydroglucose repeat unit promotes the formation of cholesteric mesophases; i.e., the order in the liquid crystal is characterized by a helicoidal supramolecular arrangement. The latter confers striking optical properties to the solution, for instance the reflection of circularly polarized light at a wavelength related to the pitch of the helicoidal arrangement.[10] Investigations have been devoted to the cholesteric phases of aqueous HPC, with emphasis on their optical properties,[11–14] their textures,[13,15–17] the comparison with theoretical predictions,[3,11] or the preparation of

0024-9297/89/2222-2286$01.50/0